

Evidence for Faradaic Processes in Scanning Probe Microscopy on Mica in Humid Air

Fardad Forouzan and Allen J. Bard*

Department of Chemistry and Biochemistry, The University of Texas at Austin, Austin, Texas 78712

Received: August 21, 1997; In Final Form: October 5, 1997[⊗]

High-resolution electrochemical deposition of silver nanostructures on insulating atomically flat mica surfaces in humid air was achieved with a scanning tunneling microscope (STM) operating in a scanning electrochemical microscopy mode. The current is faradaic and flows between the tip and a surface contact on the mica substrate through a thin water layer on the mica surface. The thickness and conductivity of the water layer governs the magnitude of the faradaic current. Modified low current STM and conventional tungsten STM tips were used for the silver deposition. The tip was held at a negative bias of -1.2 to -1.4 V (tip vs substrate), with setpoint currents of 1 – 1.7 pA. The sizes and shapes of the nanostructures were controlled by the tip scan rates and were restricted to the scan areas under the tip.

Introduction

The scanning tunneling microscope (STM) has been used to image and modify the surfaces of conducting and semiconducting materials.^{1,2} High-resolution modification of conducting surfaces^{3,4} or of adsorbed species on conducting surfaces⁵ has been achieved; however, the mechanism for these modifications is often not clear. Imaging or modification of insulating materials with the STM is usually not possible, because of the lack of a tunneling path between tip and substrate. Typically, STM studies of insulating material require coating the surface of the sample with very thin conductive layers.⁶

In a recent study, Guckenberger et al. demonstrated DNA imaging on atomically flat mica in humid air. They suggested that their images were obtained via electron tunneling through an ultrathin water film covering the sample to a metal contact distant from the tip.⁷ We later proposed⁸ that imaging occurred by a scanning electrochemical microscopy (SECM) mode⁹ in which the water layer covering the insulating substrate had sufficient ionic conductivity to permit picoampere currents to flow at the tip and contact under high-bias voltages. Under suitable conditions, a current flow between the biased tip (the working electrode) and substrate (the counter electrode) is maintained, for example, by water reduction ($2\text{H}_2\text{O} + 2\text{e}^- \rightarrow \text{H}_2 + 2\text{OH}^-$, negative tip) or water oxidation ($2\text{H}_2\text{O} \rightarrow \text{O}_2 + 4\text{H}^+ + 4\text{e}^-$, positive tip) or tip oxidation ($\text{W} + 3\text{H}_2\text{O} \rightarrow \text{WO}_3 + 6\text{H}^+ + 6\text{e}^-$, positive tip). However, Guckenberger et al.¹⁰ continued to prefer the tunneling mechanism with the STM tip not in contact with the water layer. Recently Patel et al.¹¹ in imaging proteins proposed that a water bridge exists between the tip and sample surface. A clear way to distinguish these pathways is by demonstrating that the tip current is a faradaic one (that is, it causes an oxidation or reduction reaction to occur) by observing a product of the electrode reaction. In this communication we show that silver deposition, by the reduction of $\text{Ag}(\text{I})$, occurs on a mica surface in humid air during the passage of tip currents to form small islands of silver metal. In the process, we also describe how this operational mode can be used to produce nanometer-size metallic features on the insulating mica surface.

SECM has previously been used to produce metal features.^{12–14} For example, metallic silver metal can be deposited in thin layers of the ionically (but not electronically) conductive polymer

Nafion on a metallic surface.¹² It has been established that the smallest conductive features produced on the insulating surface by SECM is of the order $0.1a$, where a is the SECM tip radius.¹⁵ The use of sharp STM tips that do not have an insulating sheath (as required for STM depositions on substrates covered by thick layers of solution)^{16–18} opens the possibility of the deposition of smaller features on insulators that can form thin ionically conductive liquid layers.

Experimental Section

Chemicals. Cr (99.95%, Alfa Aesar, Ward Hill, MA), Au (99.99%, Goodfellow, Cambridge, England), 0.01 in. diameter tungsten rod (99.99%, FHC, Brunswick, ME), silver nitrate (99.9%, MDM Scientific and Chemical, Houston, TX), and potassium hydroxide (85%, EM Scientific, Gibbstown, NJ) were used as received. Mica (Spruce Pine Mica Co., Spruce Pine, NC) was freshly cleaved prior to vapor deposition of a gold contact (Cr underlayer) from separate tungsten boats. Milli-Q water (18 M Ω , Millipore Corp., Bedford, WA) was used in all experiments. The silver nitrate solutions were prepared prior to each sample treatment and kept in the dark at all times.

Instrumentation. STM tips were prepared electrochemically by etching tungsten rods (0.01" diameter) in 1 M KOH at 30 V ac. The etched tips were rinsed with Millipore water followed by acetone and were then air-dried. A Nanoscope III (Digital Instruments, Santa Barbara, CA) STM was used with a picoamp head stage, tip view adapter ring, picoamp booster stage, and a type G atomic force microscope (AFM) scanner with a maximum X – Y directional movement of about $65 \mu\text{m}$. The picoamp head stage contained an OPI58A operational amplifier that is sensitive to static electricity. Extra caution was taken to prevent static buildup. The head stage was placed in a Teflon chamber containing a bed of molecular sieve to prevent water condensation on the circuit board. This was necessary to prevent any damage to the electronic circuitry due to water condensation and therefore shorting of the electronic components of the picoamp head stage. The sample and the stage were shielded with a cylindrical Cu mesh Faraday cage connected to the STM system ground. Since the sample had to be kept at a constant and defined relative humidity (RH), a Plexiglas environmental chamber capable of maintaining a given RH over long periods was constructed. This chamber housed the entire STM stage including the mica sample, AFM base, and G scanner. An HMI

[⊗] Abstract published in *Advance ACS Abstracts*, November 15, 1997.

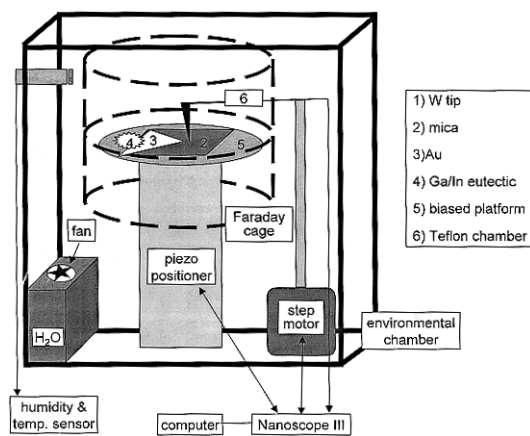


Figure 1. Schematic of the picoamp STM setup. The mica sample was maintained under constant humidity by flowing humid air in a closed environmental chamber. The connection between the Au layer on mica and the STM base was made with Ga/In eutectic.

32 meter (Vaisala, Finland) was used to measure the humidity and temperature inside the chamber. Humidity was regulated by switching on or off an electric fan positioned over a water reservoir located inside the chamber while also adjusting a vent located on the side of the environmental chamber. A simplified schematic of the STM setup used is presented in Figure 1. The environmental chamber was positioned on a platform suspended by bungee cords to minimize vibrations. An environmental scanning electron microscope, Electroscan E3 (Division of Philips Electronic Instruments Company, Wilmington, MA), was used to obtain SEM pictures. Electron spectroscopy for chemical analysis (ESCA) was carried out with a Physical Electronics PHI 5700 instrument with an Al X-ray source.

Procedures. Contact to the mica surface was made by a Au film. A 750 Å Cr underlayer was vapor deposited on freshly cleaved mica to provide good adhesion for the 3000 Å Au layer subsequently deposited. Before each experiment, part of the vapor-deposited Cr/Au layer was peeled from the mica surface with a thin strip of adhesive tape. This resulted in a clean metal/mica junction that was later used to engage the STM tip on the mica surface. Au layers (3000 Å) directly vapor deposited onto mica, without the Cr underlayer, were also used. These layers were easier to peel but would sometimes flake off during mica handling.

The modified STM in a Faraday cage was capable of detecting currents in the picoampere range. The coarse tip approach mechanism provided adequate indication of the tip nearing a conductive substrate, allowing STM imaging of conductive material with setpoint currents as low as 0.4 pA. STM of vapor-deposited Au on mica at 10% > RH > 98% showed minimal loss in image resolution as a function of increasing RH. This agrees with observations made by others.¹⁹ Atomic force microscopy of water on mica with nanometer resolution shows that at RH > 45% a uniform molecularly thin film water layer forms at 21 °C.²⁰ An increase in surface roughness of atomically flat Au terraces immobilized with the enzyme catalase has been observed as a function of RH with STM.²¹ A surface roughness of 0.14 nm at near 0% RH up to 0.42 nm at 86% RH was observed on these samples with the roughness plateauing at RH > 86%.

A suitably thin water layer thickness (a few monolayers) could be formed on the mica by careful control of the humidity and temperature in the environmental chamber. The water layer thickness formed under these conditions (on the order of 10–15 Å)¹⁹ was ideal for the silver reduction experiments. Direct engagement of the STM tip in such a thin water layer proved

very difficult. The inherent problem was that the thickness of the water layer was less than the shortest tip-to-substrate coarse approach step (about 50 nm) taken by the Nanoscope AFM base. This would cause the tip to regularly crash into mica upon direct approach.

It was better to carry out the coarse approach on the Au layer adjacent to the mica surface and then laterally move the tip onto mica via the piezoelectric positioner in the G scanner. The G scanner was capable of sufficiently large X – Y movement (about $65 \times 65 \mu\text{m}$) to allow the tip to be moved reasonably far from the sharp Au/mica interface. When the tip was moved onto the water layer-covered mica, the potential applied to the piezoelectric positioners would increase, thus moving the tip closer to the sample on the angstrom scale until the desired setpoint current was achieved. This very gradual approach minimized the tip crashes we experienced on conventional STM approach. If a nonuniform water layer covered the mica sample, the tip showed large fluctuations in the Z direction and eventually crashed into the sample.

We also attempted to produce thicker water layers by making the mica surface more hydroscopic, treating freshly cleaved mica samples with aqueous 10 mM KOH solution for 10 s followed by N₂ flow drying. These samples could be imaged in humid air by SECM, but showed random coverage by 10–50 nm diameter KOH crystals. Upon exposure to high humidity, a thick water layer (> 150 nm) uniformly covered the surface, which strongly perturbed surface imaging. In general, this treatment was not useful in preparing mica samples for thin layer experiments.

Results and Discussion

Adsorption of Silver Cations and Electrodeposition on Mica. When freshly cleaved mica is exposed to solutions of various metal cations, such as those of Sr²⁺ and Cs²⁺, ion adsorption and structure-specific ion exchange occur.^{22,23} Thus when we treated freshly cleaved mica in the dark at room temperature with 0.1 M AgNO₃ for 24 h, Ag⁺ was adsorbed on the mica surface. All experiments were done with minimal light exposure to decrease any risk of silver ion photoreduction.

To demonstrate Ag⁺ adsorption and electrodeposition of metallic Ag, the adsorption step was carried out on a piece of mica with two Au contacts spaced about 3 mm apart. These contacts were made by peeling off a 3 mm wide vapor-deposited gold layer with adhesive tape. The mica was washed with water and air-dried. When the mica was maintained at a relative humidity above 80% at 25 °C and a dc voltage of about 9 V was applied between the two contacts, a bright metallic film observable under a microscope grew with time at the cathode. This was shown to be Ag⁰ by ESCA, as described below. The currents that flowed in these experiments were on the order of picoamperes and were limited by the conductivity of the thin water layer.

We would also occasionally see irregular and somewhat dendritic silver patterns growing from the gold contacts suggesting that the silver adsorbed nonuniformly on the mica surface. The SECM experiments discussed below also suggested the existence of nonuniform adsorbed silver areas, since no silver reduction took place at some locations under the same conditions for deposition at other spots. In these cases, the negatively biased STM tip would simply engage in the water layer covering the sample and maintain a small electrolysis current. Increasing the setpoint current or decreasing the bias voltage would cause the tip to crash.

Electrodeposition of Silver on Mica by SECM. To deposit silver nanostructures, the STM tip was engaged on a AgNO₃-

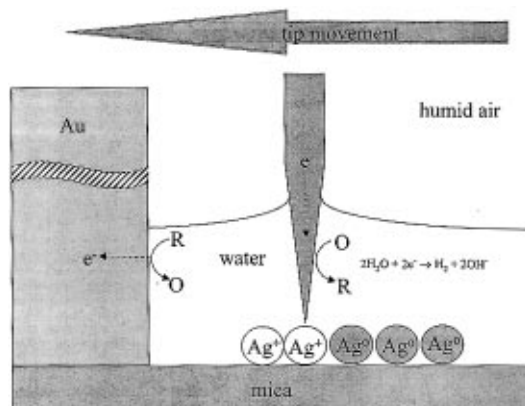


Figure 2. Schematic representation of the proposed electrochemistry taking place within the thin water layer covering the silver nitrate treated mica sample. The mica sample depicts adsorbed Ag^+ , which is reduced to Ag^0 when the tip is biased more negative than the reduction potential of Ag^+ . Water reduction is a competing reaction at the tip and water oxidation occurs at the Au contact.

treated mica sheet with a small gold contact as described above. The tip was made the cathode by negatively biasing it with respect to the Au. It was of crucial importance to keep the water layer on the mica surface thin and uniform enough to achieve and maintain tip engagement. At room temperature, a relative humidity between 80% and 95% was necessary to form the desired water layer thickness. A schematic representation of the assumed process is shown in Figure 2. At lower relative humidities, the water layer would exist as small islands, so that the mica surface did not have sufficient conductivity;²⁰ under such conditions, the tip would crash into the mica. Tip crashing would also take place when the setpoint current was set higher than that maintainable by electrolysis of the thin water layer and when the magnitude of the bias voltage was less than 0.95 V.

Figure 3 is an SEM image of a mica sample on which silver nanostructures were formed electrochemically by the above procedure. These structures were formed by applying a potential of -1.25 V (tip vs substrate) to an atomically sharp STM tip while maintaining a setpoint current of 1.4 pA at RH = 90%. The setpoint current represents the overall water and silver reduction currents at the tip and is limited by the conductivity of the water layer. The square shaped structures A, B, and C were formed with a tip scan rate of 2 Hz while the circular structure D was formed when the tip was scanned at 0.1 Hz with an applied scan of 200×200 nm. Usually the only structures that would form were square-shaped ones because they were limited by the available Nanoscope III tip movement with silver deposition under the tip. The circular structure (D) was formed when silver reduction took place at a higher rate than that achievable at slow scan rates (0.1 Hz). Such structures were never found with control mica samples that were treated with 0.1 M AgNO_3 for 24 h and were either imaged immediately or exposed to light (1600 W xenon lamp) for 3 h. These SEM images were obtained at 15 kV in an environmental SEM which is more suitable for images of nonconductive samples as it minimizes charging of the insulating samples due to electron bombardment. We do, however, see random dark spots on the image that are a result of mica charging. Prior to SEM, the sample was thoroughly rinsed with distilled deionized water and allowed to dry in a covered beaker to prevent settling of dust particles on the sample. Scanning the STM tip over smaller areas (5×5 to 25×25 nm) typically showed a very stable SECM feedback response as observed when scanning the tip during silver deposition over larger areas. However, we were

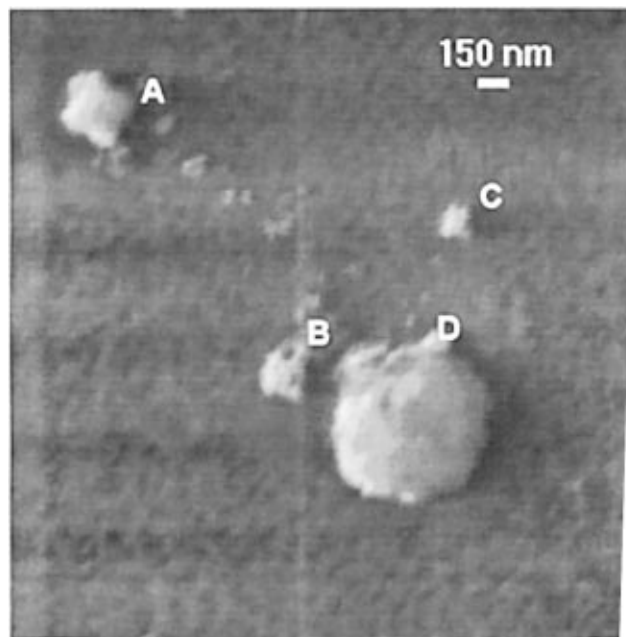


Figure 3. SEM of silver deposited patterns on a treated mica sample at RH = 90%. The square Ag deposits are (A) 350, (B) 250, and (C) 150 nm in length and are limited by the tip scan area. The circular silver deposit (D) has a radius of about 500 nm and is a result of a silver reduction rate faster than that covered under the scanned area under low tip scan rates (0.1 Hz). The applied bias was -1.25 V (tip vs substrate) and the setpoint current was 1.4 pA.

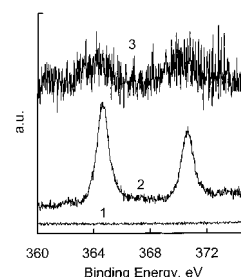


Figure 4. ESCA obtained with Al X-ray source of (1) freshly cleaved mica, (2) electrochemically reduced silver macrostructures on mica, and (3) electrochemically reduced silver nanostructures on mica with our modified STM apparatus. The Y scale is arbitrary.

unable to locate these small deposits due to SEM limiting resolution. We were unable to image the deposits by retracing them with the same STM tip used in the reduction process as soon as the deposition step was over. The Nanoscope III would repeatedly lose tip engagement probably due to the perturbation of the thin water layer during the reduction step.

Elemental analysis by ESCA showed these nanostructures to be metallic silver. Figure 4 shows ESCA scans of different samples from 360 to 375 eV, the region of the known silver $3d_{5/2}$ and $3d_{3/2}$ peaks at 368.3 and 374 eV, respectively.²⁴ Both Ag(I) and metallic silver produce peaks in this region. However, residual Ag(I) on the mica could be removed by soaking the samples in 0.1 M KNO_3 for at least 15 min and then washing with water. Mica treated with AgNO_3 , washed and dried, and then subjected to the KNO_3 treatment did not show ESCA signals for Ag above the background level of untreated mica (curve 1). A problem in the ESCA analysis is the charging of the insulating mica, causing the peaks to shift to lower binding energies compared to literature values. This occurred even under continuous irradiation with an electron gun in the ultrahigh vacuum chamber. Thus, we typically found the Ag peaks at 364.5 and 370.5. These are clearly shown (Figure 4, curve 2) for freshly cleaved mica that was treated with AgNO_3 for 24 h

and had large ($20 \times 100 \mu\text{m}$) silver areas electrochemically deposited on it, as described in the first section of the Results and Discussion Section. A scan made of mica areas with silver nanostructures deposited by the SECM mode (curve 3) showed peaks at the same energies, but with very low signal-to-noise. The samples that produced curves 2 and 3 were washed with 0.1 M KNO_3 before the analysis.

Conclusions

We have demonstrated that fabrication with an STM on insulating mica surfaces (1) requires surface coverage by a few water monolayers and (2) involves faradaic currents and hence occurs by an electrochemical (SECM) mode rather than by tunneling. The electrochemical deposition of metallic silver on the insulating surface was demonstrated and square-shaped silver structures as small as $150 \times 150 \text{ nm}$ to $350 \times 350 \text{ nm}$ were produced. The STM tip could not remain engaged on the mica surface and would crash if the applied potential between tip and substrate was not sufficiently negative to reduce water. Tip crashing would also occur if the setpoint current was set higher than that maintainable by the rate of water and silver reduction. This indicates that currents observed under these conditions are faradaic and not tunneling ones.

Acknowledgment. The support of this work by grants from the Robert A. Welch Foundation and the National Science Foundation (Grant CHE9508525) is gratefully acknowledged.

References and Notes

- (1) Pontifex, G. H.; Zhang, P.; Wang, Z.; Haslett, T. L.; AlMawlawi, D.; Moskovits, M. *J. Phys. Chem.* **1991**, *95*, 9989–9993.
- (2) Ehrichs, E. E.; Silver, R. M.; de Lozanne, A. L. *J. Vac. Sci. Technol.* **1988**, *6*, 540–543.

- (3) McCarley, R. L.; Hendricks, S. A.; Bard, A. J. *J. Phys. Chem.* **1992**, *96*, 10089–10092.
- (4) Dunlap, D.; Smith, S.; Bustamante, C.; Tamayo, J.; Garcia, R. *Rev. Sci. Instrum.* **1995**, *66*, 4876–4879.
- (5) Dujardin, G.; Walkup, R. E.; Avouris, Ph. *Science* **1995**, *255*, 1232–1235.
- (6) Jaklevic, R. C.; Elie, L.; Shen, W.-D.; Chen, J. T. *J. Vac. Sci. Technol.* **1988**, *6*, 448–453.
- (7) Guckenberger, R.; Heim, M.; Cevec, G.; Knapp, H. F.; Wieggrabe, W.; Hillebrand, A. *Science* **1994**, *266*, 1538–1540.
- (8) Fan, F.-R. F.; Bard, A. J. *Science* **1995**, *270*, 1849.
- (9) Bard, A. J.; Fan, F.-R. F.; Kwak, J.; Lev, O. *Anal. Chem.* **1989**, *61*, 132–138.
- (10) Guckenberger, R.; Heim, M. *Science* **1995**, *270*, 1851.
- (11) Patel, N.; Davies, M. C.; Lomas, M.; Roberts, C. J.; Tendler, S. J. B.; Williams, P. M. *J. Phys. Chem. B* **1997**, *101*, 5138–5142.
- (12) Craston, D. H.; Lin, C. W.; Bard, A. J. *J. Electrochem. Soc.* **1988**, *135*, 785–786.
- (13) Hüssler, O. E.; Craston, D. H.; Bard, A. J. *J. Electrochem. Soc.* **1989**, *136*, 3222–3229.
- (14) Hillier, A. C.; Ward, M. D. *Anal. Chem.* **1992**, *64*, 2539–2554.
- (15) Bard, A. J.; Mirkin, M. V.; Unwin, P. R.; Wipf, D. O. *J. Phys. Chem.* **1992**, *96*, 1861–1868.
- (16) Fan, F.-R. F.; Bard, A. J. *J. Electrochem. Soc.* **1989**, *136*, 3216–3222.
- (17) Itaya, K.; Sugawara, S. *Chem. Lett.* **1987**, 1927–1930.
- (18) Itaya, K.; Higaki, K.; Sugawara, S. *Chem. Lett.* **1988**, 421–424.
- (19) Leggett, G. J.; Davies, M. C.; Jackson, G. E.; Roberts, C. J.; Tendler, S. J. B.; Williams, P. M. *J. Phys. Chem.* **1993**, *97*, 8852.
- (20) Hu, J.; Xiao, X.-D.; Ogletree, D. F.; Salmeron, M. *Science* **1995**, *268*, 267–269.
- (21) Parker, M. C.; Davies, M. C.; Tendler, S. J. B. *J. Phys. Chem.* **1995**, *99*, 16155–16161.
- (22) Paulus, W. J.; Komarneni, S.; Roy, R. *Nature* **1992**, *357*, 571–573.
- (23) Komarneni, S.; Roy, R. *Science* **1988**, *239*, 1286–1288.
- (24) Moulder, J. F.; Stickle, W. F.; Sobol, P. E.; Bomben, K. D. *Handbook of X-ray Photoelectron Spectroscopy*, Chastin, J., King, R. C., Jr., Eds.; Physical Electronics, Inc.: Eden Prairie, MN, 1995; pp 120–121.